Pyramids and cascades: a synthesis of food chain functioning and stability

Matthieu Barbier and Michel Loreau
(Dated: July 3, 2018)

Food chain theory is one of the cornerstones of ecology, providing many of its basic predictions, such as bottom-up and top-down control, biomass pyramids, trophic cascades and predator-prey oscillations. Yet, ninety years into this theory, the precise conditions under which these patterns may occur and persist in Nature remain subject to debate. Rather than address each pattern in isolation, we propose that they must be understood together, calling for the synthesis of a fragmented set of theories and empirical results. To do this, we propose a minimal theory that combines the energetic and dynamical approaches to food chains. We chart its predictions on a concise map, where two main regimes emerge: one regime characterized by pyramidal patterns, the other by cascade patterns, across a diversity of functioning and stability metrics. The axes of this map are governed by essential physiological and ecological variables, such as metabolic rates and self-regulation. A quantitative comparison with data sheds light on conflicting theoretical predictions and empirical puzzles, from inverted size spectra to causes of trophic cascade strength. We conclude that drawing systematic connections between stability and functioning properties is a necessary step toward testing food chain theory as a reliable description of real ecosystems.

INTRODUCTION

The concept of food chain, since its formulation by Elton [1], has become one of the most widely studied in empirical and theoretical ecology [2]. It provides basic concepts for our understanding of many ecological phenomena, such as the pyramidal distribution of biomass over trophic levels, and the dynamics of predation, from population cycles to trophic cascades [3].

Yet, these fundamental patterns have a checkered history of success outside of textbook examples. When they are not observed, it is unclear whether this is because their theoretical requirements are not met, or due to mechanisms beyond the scope of food chain theory, such as complex interactions or spatial fluxes [4–11]. Even when these patterns *do* appear in empirical data, recent studies suggest that they might not truly convey information about the underlying trophic structure [12–15].

This lack of consensus may be due to an increasing fragmentation of the literature, with an originally interconnected set of structural, functional and dynamical properties growing into separate topics of investigation. Rather than studying biomass pyramids or trophic cascades in isolation, we argue that combining multiple lines of evidence will prove crucial to truly assess the empirical support for food chain theory.

Empirical validation first requires unequivocal theoretical expectations, but two distinct paradigms have come to shape how we understand food chains and predict their behaviors. The *energetic* paradigm follows Hutchinson and Lindeman [16] in focusing on the macroscopic distribution of energy, and its flow up the food chain. It has remained tightly bound to large-scale empirical studies, especially of biomass pyramids and size spectra in aquatic ecosystems [17–19]. The *dynamical* paradigm follows Lotka and Volterra [20, 21] in describing predation impacts down the chain. It emphasizes individual species, the role of consumers, and mathematical models of time series and their stability [22]. While these two paradigms may seem to have different purviews, there is a number of shared topics on which their predictions appear to clash: for instance, biomass pyramids often fail to emerge in dynamical models [23]. We believe that these theoretical approaches can and must be embedded within a single framework.

This systematic viewpoint has been argued for at a conceptual level [24] but it has yet to coalesce into a quantitative formalism: a concise map of all essential food chain behaviors and their interplay, along with the key ecological parameters that govern them.

As a first step toward this synthesis, we propose a minimal model built from the ingredients of the two paradigms. They are found to occupy opposite corners in a unified parameter space, as they make conflicting assumptions about the role of various ecological mechanisms, from self-regulation to metabolic scaling.

We chart basic functioning and stability patterns across that unified parameter space. We predict the distribution of biomass and production, as well as the response to various perturbations, from harvesting or predator removal to stochastic fluctuations. This leads us to distinguish two qualitatively different parameter regimes. In the first regime, all properties studied here exhibit pyramidal patterns. In the second, they display cascade (alternating) patterns. We will argue that this coherence between diverse properties is an important fingerprint of food chain structure.

We finally illustrate how this approach can lead to new insights into empirical data, and quantitative tests of food chain theory, before discussing both its limitations and its prospects.

Box 1: The energetic and dynamical paradigms

The *energetic* paradigm focuses on macroscopic patterns of energy distribution among trophic levels, following a widely-used heuristic formula [15, 18, 25]

$$m_i B_i = E m_{i-1} B_{i-1} \tag{1}$$

where B_i is the biomass of trophic leve i, m_i is its metabolic rate, and $m_i B_i$ is interpreted as its energy content. While E is often called the energy transfer efficiency, we show in the main text that fast consumer metabolism may allow $E > 1$.

The *dynamical* paradigm emphasizes the role of predators in regulating their prey, assumes that consumer metabolism drives trophic interactions [26], and explores the role of different functional responses [27]. The simplest is the Lotka-Volterra model:

$$\frac{dB_i}{dt} = m_i B_i(-r + \varepsilon B_{i-1}) - m_{i+1} B_{i+1}. \tag{2}$$

By embedding both paradigms in our synthetic model (see definitions in Box 2), we can highlight their differences:

	Energetic	**Dynamical**
Assumptions		
• Mortality	$r = 0$	$r > 0$
• Self-regulation[a]	Strong ($\lambda \ll 1$)	Negligible ($\lambda \gg 1$)
• Consumption rate[b]	Resource	Consumer
set by metabolism of	($\alpha_{i,i-1} \sim m_{i-1}$)	($\alpha_{i,i-1} \sim m_i$)
Predictions		
• Functioning and stability patterns	Bottom-up pyramid	Top-down cascade[e]
• Bottom-up control[c]	Donor	Antagonistic
• Biomass-productivity[c]	$B_i \sim p_i$	$B_i \sim p_{i-1}$
• Top-down feedback[d]	$\lambda \sim 1/m$	$\lambda \sim m$
• Metabolic ratio[d]	$m > 1$ stabilizing	$m < 1$ stabilizing
Evidence	Herbivory data	Tritrophic chain data

[a] See Fig. 1. [b] See (8). [c] See (11) and (12). [d] $m = m_i/m_{i-1}$, hence $m > 1$ means faster predator than prey metabolism.
[e] *Cascade* designates alternating patterns of positive and negative, or high and low, values across trophic levels.

A SYNTHETIC MODEL

Key ingredients

The two theoretical paradigms that we synthesize (Box 1) involve a common set of fundamental ecological parameters used throughout this study: primary productivity (growth of the basal autotrophs) g [28], the average ratio of body masses M or metabolic rates m between predator and prey [26], the physiological conversion efficiency of resources into consumer biomass ε [29], and the strength of interactions between and within species [30, 31], which we denote by α and D, respectively, and which we combine into the ratio $a = \alpha/D$.

We propose the simplest food chain model that includes these parameters and reproduces the predictions of the two paradigms (Box 2). The behavior of the simple chain (3) depends on the rates at which biomass is generated at the basal level, transfered to higher levels and lost to inefficiencies, metabolic costs and mortality.

To understand basic biomass and stability patterns in this model, let us first consider the case where every activity of a trophic level (growth, mortality, competition and uptake) occurs on related timescales, sharing a common factor m_i, which we interpret as a characteristic metabolic rate. With this choice, the same coefficients appear at all levels in the equilibrium condition (6) of our model, giving a clear role to each of the ecological parameters listed above.

In the Discussion, we address non-linear functional responses, and how self-regulation D_i can derive from consumer interference. We also consider how the results of this basic model may extend to more complex food webs.

Connecting the paradigms

By comparing the energetic formula (1) in Box 1 with the equilibrium of our model (6) in Box 2, we notice that the former effectively neglects all losses, and retains only self-regulation and the energy influx from consumption. In that identification, the energy ratio between levels is $E = m\varepsilon a$, and it is thus possible to have $E > 1$ (an inverted energy pyramid). By contrast, the dynamical model (2) emphasizes predation losses and neglects the self-regulation term: we will see below that this choice corresponds to $\lambda = m\varepsilon a^2 \gg 1$, while neglecting predation corresponds to $\lambda \ll 1$ (Fig. 1).

Hence, the first discrepancy between the two paradigms lies in the role of self-regulation D_i, which is central, if implicit, in the energetic argument, yet often absent from dynamical models. This may reflect

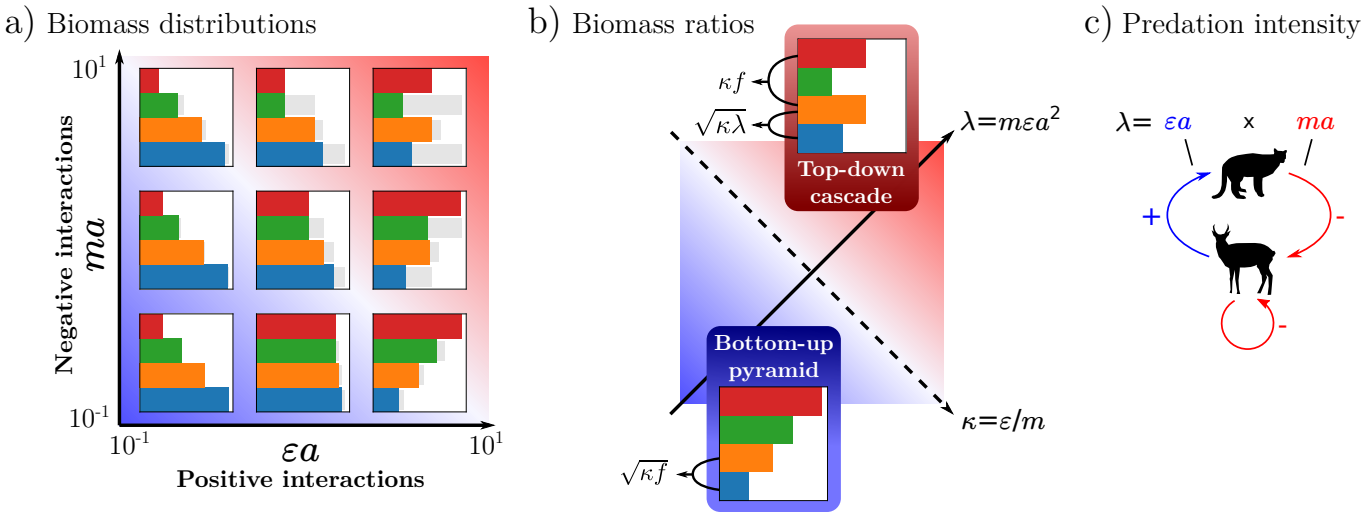

FIG. 1. Map of biomass patterns in a food chain. The parameters are predator-prey metabolic ratio m, conversion efficiency ε and the effective strength of interactions a (Box 2). Note that a may itself be a function of m per (8). Results are illustrated for a four-level chain with negligible mortality $\rho \ll 1$ (other examples in Supporting Information). **a)** Biomass distribution. For each trophic level, a colored bar represents its equilibrium biomass (in log scale), and a grey bar represents the amount of biomass lost to its predator, reflecting the intensity of top-down control. **b)** Parameters that govern the slope of the biomass distribution. The main diagonal $\lambda = m\varepsilon a^2$ distinguishes the region of bottom-up control $\lambda < 1$ with pyramids (both regular and inverted), from the region of top-down control $\lambda > 1$ with cascades. The other diagonal $\kappa = \varepsilon/m$ affects the top-heaviness of the biomass distribution (we show in Fig. 3 and 4 that it has no effect on the dynamics). As explained in the main text, the general slope of the distribution is given by $B_{i+2}/B_i \sim \kappa f$ with f the fraction of production removed by predators (17). In pyramids, we thus find $B_{i+1}/B_i \sim \sqrt{\kappa f}$, while in cascades, we see an alternation between low-biomass and high-biomass levels i and $i+1$ with $B_{i+1}/B_i \sim \sqrt{\kappa\lambda} = \varepsilon a$ (which may be significantly larger than the pyramid slope). **c)** The parameter λ represents the intensity of feedback of a trophic level on itself through its predators: how much one unit of prey biomass increases predator biomass at equilibrium (εa), times how much this additional predation suppresses the prey (ma), compared to self-regulation. Losses from predation can thus be neglected if $\lambda \ll 1$, while self-regulation is negligible if $\lambda \gg 1$.

the difference between a macroscopic viewpoint, where a trophic level is generally found to coexist with the (often more abundant) level below, and a microscopic viewpoint where a predator species may dramatically deplete its prey species in a small locality. Yet, even locally, empirical evidence suggests the underestimated role of self-regulation in the form of predator interference [31].

The second difference is that energetic models generally assume negligible energy loss through metabolism and mortality, $\rho = r/g \ll 1$ (see Box 2). In that limit, basal growth (primary productivity) g plays no role in the dynamics, only setting the scale for the total biomass in the system. By contrast, the dynamical paradigm assumes significant losses ρ, and thus assigns a major role to basal growth g, whose increase can rescue less abundant consumers. This leads most notably to the paradox of enrichment [27].

The third difference lies in the rate of consumption. Dynamical models again adopt the consumer's perspective: a predator with a faster metabolism is expected to have a higher attack rate, hence the consumption rate $\alpha_{i,i-1}$ scales with the *consumer*'s metabolism m_i. On the other hand, energetic models assume that consumption – or energy influx, the right-hand term in (1) – scales with the metabolic rate of the *resource*. To encompass both approaches, we can assume a generalized scaling

$$\alpha_{i,i-1} \sim m_i^{\nu}(m_{i-1})^{1-\nu}, \qquad a = \frac{\alpha_{i,i-1}}{D_i} \sim m^{\nu-1} \tag{8}$$

The resource-driven (energetic) viewpoint is given by $\nu = 0$ (and hence, $\lambda \sim 1/m$), and the consumer-driven (dynamical) one by $\nu = 1$ ($\lambda \sim m$), see Box 1.

As a result of these conflicting assumptions, we expect the two paradigms to emphasize either bottom-up pyramids or top-down cascades, but also to make different predictions about the role of primary productivity and metabolic scaling.

Bottom-up and top-down control

The fundamental dynamical mechanism that gives rise to all food chain patterns is the interplay between bottom-up and top-down control. However, the energetic and the dynamical paradigms have conflicting notions of what is meant by bottom-up control.

Consider a two-level chain as an illustration. In the absence of any self-regulation, setting $D_i = 0$ in (3), the

Box 2: Basic food chain model and key parameters

We propose the simplest model that can reproduce the predictions of both energetic and dynamical paradigms (Box 1)

$$\frac{dB_i}{dt} = B_i \left(g_i - D_i B_i + \varepsilon \alpha_{i,i-1} B_{i-1} - \alpha_{i+1,i} B_{i+1}\right) \tag{3}$$

where B_i is the biomass of trophic level i, ε is the biomass conversion efficiency, and α_{ij} the interaction strength. Demographic processes, both density-independent (g_i) and dependent (D_i), are assumed to scale with the species' metabolic rate m_i:

$$D_i = m_i D, \quad g_i = m_i \begin{cases} g & i = 1 \text{ (autotrophic growth)} \\ -r, & i > 1 \text{ (consumer mortality)} \end{cases} \tag{4}$$

Note that the autotroph carrying capacity g_1/D_1 sets the scale for the total biomass in the chain. To allow direct comparison between density-dependent and independent terms, we can choose biomass units such that $g = D$. The model further simplifies if the predator-prey metabolic ratio and the ratio of interaction strength to self-regulation

$$m = m_{i+1}/m_i, \qquad a = \alpha_{i,i-1}/D_i \tag{5}$$

are both constant throughout the chain. Note that interactions can depend on metabolism in various ways, so a may be a function of m, see (8). The equilibrium condition for surviving consumers ($i > 1$) is then

$$0 = \underbrace{-\frac{r}{g}}_{\text{linear loss}} - \underbrace{B_i}_{\text{self-regulation}} + \underbrace{\varepsilon a B_{i-1}}_{\text{consumption}} - \underbrace{m a B_{i+1}}_{\text{predation loss}} \tag{6}$$

where we see that the energetic formula (1) ignores linear and predation loss and retains only self-regulation and consumption. The solution (see Appendix S1 in Supporting Information) depends on three synthetic parameters:

$$\rho = \frac{r}{g}, \qquad \lambda = m\varepsilon a^2, \qquad \kappa = \frac{\varepsilon}{m} \tag{7}$$

Two of these parameters shape the main qualitative behaviors: energy flux up the chain κ, and top-down feedback λ (predation losses are negligible if $\lambda \ll 1$) as shown in Fig. 1. By contrast, ρ does not create new patterns, but can push trophic levels to extinction. This distinguishes two possible scenarios, depending on whether food chains are limited by energy losses (large ρ) or not (small ρ). In the second case, basal growth g disappears from (6) and only intervenes as a scaling factor in the biomasses.

chain reaches the equilibrium

$$0 = g - m\alpha B_2, \qquad 0 = -r + \varepsilon \alpha B_1 \tag{9}$$

where we see that each level controls the other. Resource biomass B_1 is fixed by consumer mortality r, corresponding to top-down control (if r is small, the resource is almost driven to exhaustion). On the other hand, consumer biomass B_2 is fixed by basal growth g. This is *antagonistic* bottom-up control (Box 1), where consumers are limited by their prey in the sense that they grow until they deplete its production.

This situation persists if at least one trophic level lacks self-regulation: whether consumers or resources, that level will grow until it is limited by the antagonistic interaction, i.e. until consumers remove all prey growth and cannot grow further themselves.

It is only with self-regulation $D_i > 0$ at *both* levels that the two populations can stabilize before resource production is entirely consumed. Self-regulation thus gives rise to the classic notion of *donor* control, where a trophic level's biomass is fixed by its prey's, but does not increase enough to exert a negative impact on that prey.

One difference between these two notions of bottom-up control is the relationship between biomass B_i and productivity p_i, widely studied empirically [32, 33]. Productivity (biomass produced per capita) is given by

$$p_i = g_i + \varepsilon \alpha_{i,i-1} B_{i-1} \tag{10}$$

in (3). In a general food chain, *donor* control is characterized by coexistence and proportionality between levels,

$$B_i \sim p_i \sim B_{i-1} \tag{11}$$

as in the energetic formula (1). On the other hand, *antagonistic* bottom-up control is characterized by the fact that predator biomass grows until depleting prey production, as in (9), and thus

$$B_i \sim p_{i-1}, \qquad B_i \nsim p_i \tag{12}$$

where we expect no correlation between a trophic level's biomass and its productivity.

The prevalence of each scenario may depend both on the nature of the ecosystem and the scale considered, from micro- to macroscopic [34]. Hereafter, "bottom-up control" will be used in the donor sense, which is incompatible with top-down control, rather than in the antagonistic sense, in which trophic levels alternate between top-down and bottom-up control.

FUNCTIONING PATTERNS

We now use our model to clarify relationships between food web patterns, illustrating them for a four-level food chain in the limit of low mortality or high basal growth rates $\rho \ll 1$. This limit ensures that trophic levels cannot

go extinct, and that our description is robust to changes in food chain length or primary production. We show in Appendix S1 how our results can be extended to arbitrary mortality rates.

Biomass and production

One of the most central predictions of food chain theory is the distribution of energy among trophic levels, in the form of either biomass or growth. Since Elton [1], energetic arguments have led to expect pyramidal or hierarchical patterns (Fig. 1), but few studies have investigated when this structure can emerge dynamically [23, 35, 36].

We see in Fig. 1a that biomass patterns vary along two dimensions: ma and εa, the strength of negative and positive interactions in (6). We now argue that the diagonals represented on Fig. 1b are more significant axes. In the limit of low mortality, biomass patterns are controlled only by these synthetic parameters

$$\lambda = m\varepsilon a^2, \qquad \kappa = \varepsilon/m. \tag{13}$$

As shown in Fig. 1c, λ denotes the strength of predation feedback, i.e. how much a trophic level limits itself through its predators. For $\lambda > 1$, losses from predation play a large role in shaping the biomass distribution. The second axis, κ, indicates whether biomass accumulates toward the top or the bottom of the chain.

As in the two-level chain (9), top-down control is reflected in how much production is lost to consumers. The production (biomass created per unit time) of consumer species i in (3) is $\varepsilon\alpha_{i,i-1}B_iB_{i-1}$. Hence, the ratio

$$f_i = \frac{maB_{i+1}}{\varepsilon aB_{i-1}} = \frac{B_{i+1}}{\kappa B_{i-1}} \tag{14}$$

can be interpreted as the fraction of production at level i lost to consumer $i+1$, a quantity that can be estimated empirically for herbivory [32].

If we assume that the biomass distribution is pyramidal (constant ratio B_{i+1}/B_i), a simple calculation from (6) gives

$$B_{i+1} = \kappa f B_{i-1} \tag{15}$$

$$B_i \sim (\kappa f)^{i/2} \tag{16}$$

where we find that there is a constant fraction f of consumed production throughout the chain, which is the solution of

$$\frac{f}{(1-f)^2} = m\varepsilon a^2 \equiv \lambda. \tag{17}$$

Thus, λ and κ together define the trend of the biomass pyramid (16) toward bottom-heaviness ($\kappa f < 1$) or top-heaviness ($\kappa f > 1$), illustrated in Fig. 1: κ captures upward energy flow, and λ captures the limiting effect of consumption.

Yet we also expect that this pyramidal structure disappears for low self-regulation, as in (9). Solving the equilibrium (6) more carefully (see Appendix S1), we find that if $\lambda \gtrsim 1$, a cascade pattern emerges. The top predator (level $i+1$) removes a large fraction f_i of its prey's production, which is still equal to the solution f in (17). The top prey (level i), in turn, removes only a negligible fraction of its own prey's production. Thus, the chain alternates between high and low-biomass levels (Fig. 1a), experiencing antagonistic bottom-up and top-down control, respectively.

Even in this trophic cascade regime, the relation (15) holds approximately between levels two steps apart, and indicates the overall slope, i.e. the accumulation of biomass toward the top or the bottom of a long chain. But if trophic level $i+1$ (e.g. the top predator) exerts top-down control on level i, the biomass ratio $B_{i+1}/B_i \approx \sqrt{\kappa\lambda}$ can become much larger than the overall slope $\sqrt{\kappa f}$, since the fraction $f \leq 1$ is bounded but λ is not.

Thus, the trophic cascade regime may give the illusion of a steep inverted pyramid, holding only between adjacent trophic levels, as in the empirical example below.

Size spectrum

The distribution of energy among trophic levels is most useful when these levels are clearly distinct, e.g. in simple plant-herbivore-carnivore chains. In many systems, however, trophic height is not so easily assessed. Instead, the most immediate property of an organism is its size, especially in aquatic food webs. The study of these ecosystems thus relies on the size spectrum [18] or distribution of biomass among size classes.

The pyramidal slope (16) can be translated into a continuous spectrum as a function of body mass (or size) W_i. Furthermore, since the metabolic rate m_i is also less accessible than body size, many studies posit an allometric scaling of metabolism with size, $m_i \sim W_i^{-\beta}$ [26].

Let us define the predator-prey body mass ratio M, which is assumed to be constant throughout the chain:

$$M = \frac{W_{i+1}}{W_i}, \qquad W_i = W_0 M^i. \tag{18}$$

The trophic level i for size class W_i is thus given by $i \sim \log W_i/\log M$. By substituting this into the exponent in (16) and using the allometric scaling $m \sim M^{-\beta}$, we find the size spectrum for a continuous variable W

$$B(W) \sim W^b, \qquad b = \frac{1}{2}\left(\beta + \frac{\log(\varepsilon f)}{\log M}\right). \tag{19}$$

Previous studies [18] have used the energetic argument (1) and obtained a similar prediction, but with a different exponent: $b = \beta + \log\varepsilon/\log M$. Our formula corrects it with two terms coming from the predation feedback:

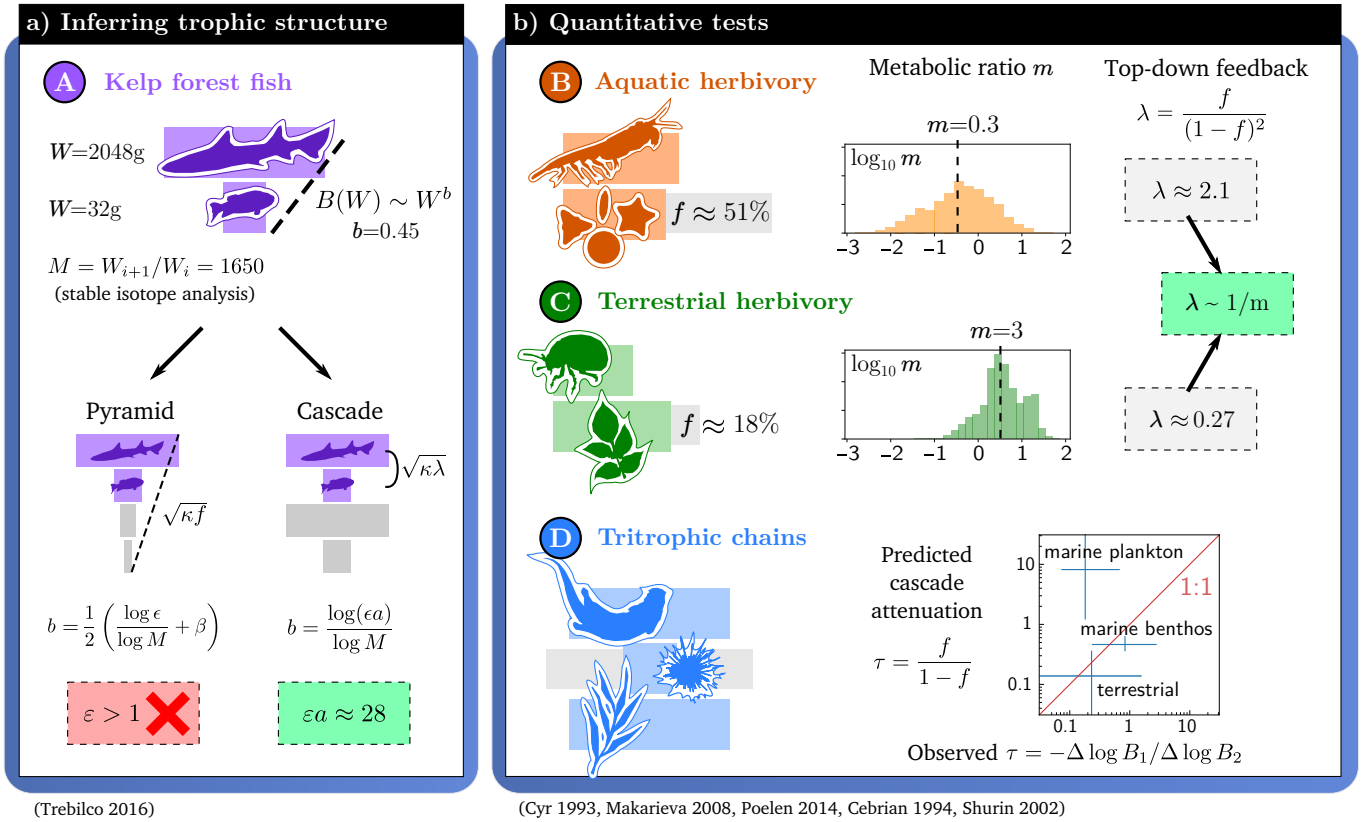

FIG. 2. Illustrating empirical challenges for a synthetic food chain theory. **a)** Identifying possible trophic structure from community patterns. Fish in kelp forests (A) exhibit a top-heavy size spectrum [37] which is incompatible with the prediction for biomass pyramids (19) except for an unphysical value of biomass conversion efficiency $\varepsilon > 1$. This apparent paradox may, however, be solved by instead assuming a cascade pattern following (20). **b)** Quantitative predictions. Aquatic herbivory (B) accounts on average for $f = 51\%$ primary production removal across various ecosystems while terrestrial herbivory (C) only removes $f = 18\%$ of production [38]. They also differ by their median metabolic ratio m, measured from the data in Fig. S3. The corresponding values of λ are compatible with the scaling $\lambda \sim 1/m$ in resource-driven consumption (8). In tritrophic chains (D), we compare empirical measurements of the trophic cascade amplification factor τ [39] to predictions using data on f for various ecosystems [32], finding plausible agreement except for marine plankton.

the fraction of production removal f, and the prefactor 1/2. We show in Appendix S1 that the two formulas coincide for resource-driven consumption (8) with strong self-regulation $\lambda \ll 1$.

From metabolic data, it is generally estimated that $\beta \in [0, \frac{1}{3}]$ [40–42]. While top-heavy pyramidal size spectra are allowed by (19), they are expected to have at most exponent $b = \beta/2 \leq \frac{1}{6}$ since $\log(\varepsilon f) \leq 0$ ($\varepsilon, f \leq 1$). For instance, in an oceanic food chain, large mammal biomass could at most exceed unicell biomass by two orders of magnitude.

A steeper slope in the spectrum may only be seen over a limited size range, between a low-biomass level and a high-biomass level in a cascade, $B_{i+1}/B_i \approx \sqrt{\kappa\lambda} = \varepsilon a$, giving

$$b = \frac{\log \varepsilon a}{\log M}. \tag{20}$$

We now show that we can use the size spectrum exponent to probe the structure of an empirical food chain.

The paradox of steep inverted size spectra

Fish in kelp forests exhibit a top-heavy size spectrum, but its slope appears steeper than allowed by energetics, leading to a paradox discussed in a recent study [37] and shown in Fig. 2a. That study measures the size spectrum $B(W) \sim W^b$ with exponent $b \approx 0.4$, suggesting an impossible efficiency $\varepsilon > 1$ in formula (19).

To solve this paradox, we first notice that the exponent b is measured over a limited size range, spanning less than two trophic levels. Indeed, the study uses stable isotope analysis to estimate the mass ratio between trophic levels, but the observed spectrum covers only body masses from 32 to 2048g (a ratio of 64 between the largest and the smallest fish). Thus, it may be misleading to analyze this spectrum as a multi-level biomass pyramid described by

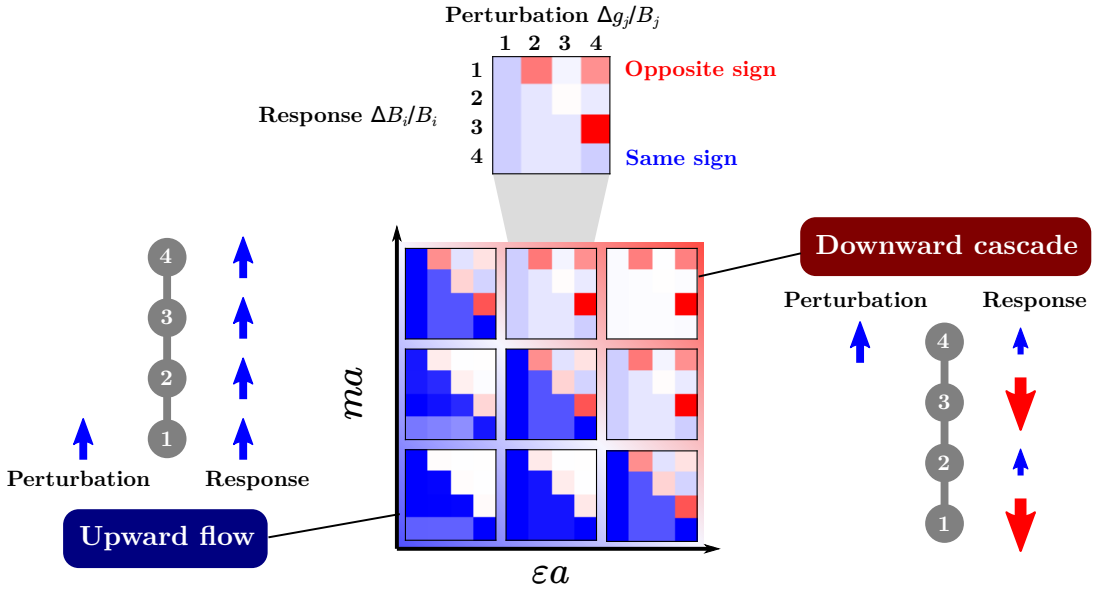

FIG. 3. Map of response to press perturbations. For various parameter values, we show the matrix V_{ij} of responses to press perturbations, as measured by the relative biomass change $\Delta B_i/B_i$ in response to a relative change of growth rate $\Delta g_j/B_j$ (see Box 3). We see here that predation feedback, the diagonal axis λ on Fig. 1, is the parameter that controls stability, while V_{ij} is constant along the other diagonal κ (this symmetry would be lost if we looked at the absolute rather than the relative response, see Fig. S1). In blue (red), we show positive (negative) response: a press on species j affects species i in the same (opposite) direction. In the bottom-left corner, responses are dominated by bottom-up propagation of the perturbation (positive effects on levels above). In the top-right corner, responses are dominated by top-down cascades (alternating effects on levels below).

formula (19).

Instead, we raise the possibility of a cascade pattern (Fig. 1), with the largest fish in the sample belonging to a high-biomass level. In that case, equation (20) allows us to infer that $\varepsilon a \approx 28$, i.e. strong interactions. Using metabolic data (see Appendix S1) we further estimate that $\lambda \gtrsim 10^3$. We predict that, in the size class with the lowest biomass (probably outside the range considered in the study), the fraction of production removed by predation should be $f \approx 97\%$. A natural test of this hypothesis would be to directly measure consumption or the strength of trophic cascades in this system.

STABILITY PATTERNS

Trophic cascades and response to a press

Trophic cascades are often studied by comparing systems where the predator is absent and present, e.g. [46]. But similar effects can also occur when predator abundance is modified by a smaller amount.

More generally, we consider a long-term decrease or increase in any trophic level's biomass, due for instance to harvesting or nutrient enrichment. It can be modelled as a press perturbation (Box 3), equivalent to a change Δg_i of the growth or mortality rate, g_i, in (3). We thus study the matrix of (relative) response $\Delta B_j/B_j$ to a press $\Delta g_i/B_i$, shown in Fig. 3.

Upward propagation of perturbations, whereby a decrease (increase) in the abundance of a trophic level leads to a decrease (increase) at all higher levels, appears as a blue lower triangle in the press response matrix in Fig. 3. This dominates the community response when $\lambda < 1$. Downward cascades are characterized by alternating negative and positive responses of the levels below the perturbed species, which appear in alternating red and blue in the upper triangle of the response matrix. They dominate when $\lambda > 1$. This qualitative shift coincides with that in the shape of the biomass distribution (Fig. 1).

Another important but counter-intuitive factor is basal growth (primary productivity) g, which discounts energy loss r in higher trophic levels. When the food chain is not limited by energy loss (small $\rho = r/g$, see Box 2), cascade strength only depends on λ, creating the consistent patterns seen in Fig. 3.

But in energy-limited food chains (large ρ), the precise value of ρ, and therefore of basal growth g, also becomes important. It may in fact play an inconsistent role in cascade effects, as we show by analyzing a three-level plant-herbivore-carnivore chain (see Appendix S1). If we add or remove the carnivore level $i = 3$ entirely, the relative change of basal biomass $\Delta \log B_1 = \Delta B_1/B_1$ indeed increases with g, as adding carnivores limits herbivory, and some of the primary production contributes to increasing the plant equilibrium biomass. By contrast, for

Box 3: Stability analysis

We study the quantitative stability properties of the model in Box 2, i.e. its response to various types of perturbations. The dynamical equation (3) becomes

$$\frac{1}{B_i}\frac{dB_i}{dt} = \xi_i(t) + g_i - D_i B_i + \varepsilon\alpha_{i,i-1}B_{i-1} - \alpha_{i+1,i}B_{i+1} \tag{21}$$

where $\xi_i(t)$ represents the perturbation.

We focus on two types of long-term perturbations. In the first case, we compute the effect of a constant press perturbation $\xi_i(t) = \xi$ on one species at a time. This can be interpreted as a permanent change Δg_i of its growth or mortality term, up to complete removal of the species. We predict the resulting change in abundance ΔN_j at each level. In the second case, we add demographic stochasticity to each species in turn, $\xi_i(t) = W(t)/\sqrt{B_i}$ with $W(t)$ a white noise term (see Appendix S1). We then compute the covariance matrix of the biomass fluctuations of all species. These two responses are connected to other stability properties, such as structural stability and return time to equilibrium [43–45].

In Fig. 3 and 4, we show results for *relative* stability metrics, rescaled by equilibrium abundances:

$$V_{ij} = \frac{\Delta B_i/B_i}{\Delta g_j/B_j}, \qquad C^{(i)}_{jk} = \frac{\mathrm{cov}(B_j, B_k)}{\mathrm{E}[B_j]\,\mathrm{E}[B_k]} \tag{22}$$

with V_{ij} the relative response of i to a press on j, and $C^{(i)}$ the relative covariance matrix between all species created by perturbing species i only. This choice reveals clear pyramidal or cascade patterns that are essentially determined by a single parameter, λ. When using absolute metrics (Fig. S1), these patterns are skewed by the biomass distribution and less apparent to the eye.

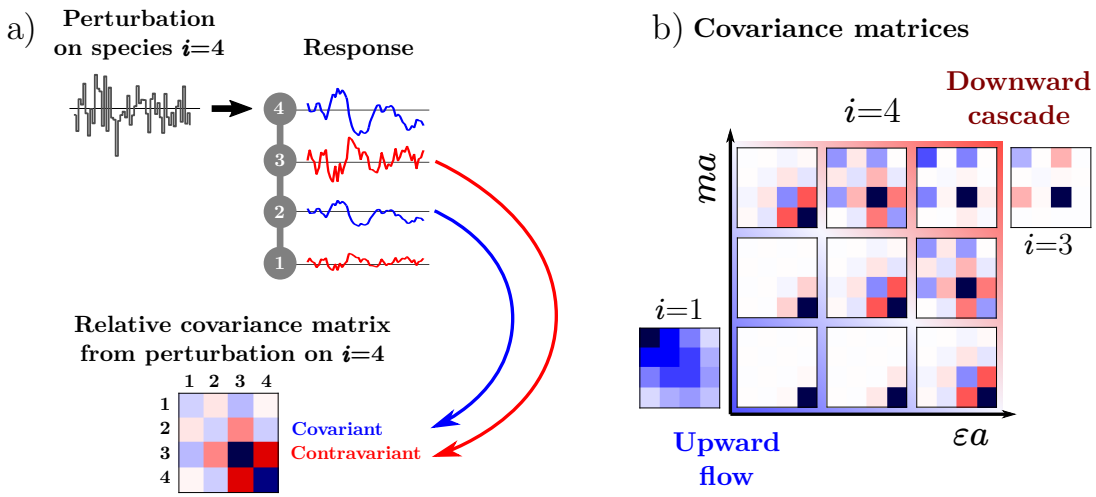

FIG. 4. Map of temporal variability under stochastic perturbations. a) We apply stochastic perturbations to species i, and measure the covariance of the time series $B_i(t)$ for all species. We show here the *relative* covariance matrix $C^{(i)}$ defined in Box 3 (blue and red indicate positive and negative covariance). The diagonal element $C^{(i)}_{jj}$ is thus the squared coefficient of variation (CV) of species j. b) Covariance patterns in the parameter space of Fig. 1. For the whole parameter space, we show covariances matrices created by perturbing the top species ($i = 4$). In the bottom-left corner ($\lambda \ll 1$), we also show the effect of perturbing the basal species ($i = 1$) and see that fluctuations only propagate upward: all species covary in the matrix $C^{(1)}$, while only species 4 fluctuates when it is the one perturbed, as shown by matrix $C^{(4)}$. In the region of top-down control ($\lambda \gtrsim 1$), perturbing each species creates a covariance cascade pattern on species below, with anticorrelated fluctuations betweeen adjacent levels. At the top-right ($\lambda \gg 1$), the matrices created by perturbing the top predator $i = 4$ and its prey $i = 3$ show a regular cascade or a two-step cascade (i.e. alternating positive and negative covariance between second neighbors). In that region, we also find an alternating pattern in the CV (on the diagonal of the matrix), with the top species being least responsive to noise and its prey being most responsive, no matter which species is perturbed.

a small perturbation of carnivore abundance, the absolute response ΔB_1 is entirely independent of g. Since the equilibrium biomass B_1 at the denominator increases with g, the log ratio $\Delta \log B_1$ decreases. Thus, enrichment may appear to correlate positively or negatively with cascade strength, depending on how the latter is measured.

The existence of two distinct regimes, with trophic cascades controlled either by g and λ, or by λ only, is further supported by the fact that nutrient enrichment (increasing basal growth g) appears to have strong effects on cascade strength in some empirical meta-analyses [5], but no significant impact in others [6].

Variability under stochastic perturbations

We also find "covariance cascades", by imposing stochastic noise on one level and looking at the variances and covariances of all levels' time series (Fig. 4). We rescale them by equilibrium biomasses to obtain a relative covariance matrix (Box 3). The diagonal elements of this matrix are the squares of the coefficients of variation (hereafter CV) of the trophic levels.

For low $\lambda \ll 1$, the trophic level with the highest CV (shown on the diagonal of the relative covariance matrix) is the one that is directly perturbed, and this perturbation propagates only to higher species, which covary positively. For intermediate $\lambda \gtrsim 1$, we see a distinct checkerboard pattern (covariance cascade) for all species below the perturbed one, reflecting the tendency of prey abundaces to fluctuate in opposition to their predators. In the top-down regime $\lambda \gg 1$, the species with the lowest CV is always the top predator, while its prey has the highest CV, and lower levels alternate between the two, similarly to well-known production and biomass patterns [3, 47].

Perturbing intermediate levels gives rise to a "two-step" covariance cascade: species two levels apart exhibit anticorrelated fluctuations. This can be interpreted as a cascade between predator-prey pairs, rather than between individual levels, due to the prey being tightly controlled by its predator.

In a dynamical model with nonlinear functional response, these anticorrelated fluctuations around equilibrium could announce the transition to more complex dynamical regimes such as oscillations or chaos. These regimes are described in a vast literature [9, 22, 48, 49], but they are expected to disappear given sufficiently strong self-regulation. It would be worthwhile to connect our near-equilibrium picture with predator-prey cycles and other dynamical food chain patterns.

EMPIRICAL EXAMPLES

Differences between aquatic and terrestrial herbivory

Food web ecology has long focused on explaining dissimilarities between aquatic and terrestrial food webs [7]. One striking difference is that aquatic herbivores consumes on average $f = 51\%$ of primary production across many ecosystems, while terrestrial herbivory only removes $f = 18\%$ of plant production [38]. This discrepancy is commonly explained by terrestrial plants having slower turnover than their consumers, while aquatic basal species, especially phytoplankton, have much faster turnover. In some systems, this allows aquatic herbivores to consume almost up to 100% of phytoplankton biomass and production each day [32].

The consistency of this explanation can be test quantitatively in our model, as we show in Fig. 2b. Using measurements on f, we can compute $\lambda = f/(1-f)$ and check that $\lambda \sim 1/m$, in agreement with the scenario of resource-driven consumption[1]. Hence, the large difference between aquatic and terrestrial values of consumed production fraction f may indeed plausibly have a physiological origin in metabolic rates.

Cascade strength in tritrophic chains

Trophic cascade strength is commonly measured empirically as the relative change in plant biomass (or plant log ratio), $\Delta \log B_1 = \Delta B_1/B_1$, in response to predator manipulation.

In a meta-analysis, the plant log ratio was found to correlate most strongly with the carnivore-herbivore metabolic ratio m_3/m_2 [10]. This correlation can be predicted in a three-level chain (see Appendix S1) under two conditions: first, the carnivore must have significant self-regulation D_3; second, its attack rate must scale with its own metabolic rate, $\alpha_{32} \sim m_3$, in agreement with consumer-driven consumption in (8) and in contrast with what was found above for herbivory.

Another salient property of cascades is whether the effect attenuates or intensifies down the chain, e.g. whether plants are less or more affected than herbivores by carnivore removal. This factor has been measured empirically, and explained by different biological mechanisms (from plant defenses to external subsidies) in a variety of systems [50]. In the three-level chain, we find

$$\tau \equiv \frac{\Delta \log B_1}{-\Delta \log B_2} = \frac{f_1}{1-f_1}, \tag{23}$$

indicating that, without the need to invoke additonal mechanisms, attenuation happens if the fraction of consumed primary production is less than half, $f_1 < 50\%$, while intensification happens otherwise.

From the data on herbivory used above, we estimate an amplification factor $\tau = f/(1-f) \approx 1$ in aquatic foodwebs, meaning that cascade effects tend to propagate without significant attenuation. By contrast, we expect fast-decaying cascades with $\tau \approx 0.2$ in terrestrial systems. In Fig. 2b, we use additional data on τ from [39] and f from [32] to show that these predictions are mostly borne out. Combined with the previous section, this is indicative evidence that metabolic rates could be a sufficient explanation for observed trophic cascade attenuation.

---

[1] We first notice that a linear relationship is found between primary production and herbivore biomass [33], i.e. $B_i \sim P_{i-1}$. This relationship is what we expect from equilibrium condition (6) in the low-mortality limit $\rho \ll 1$, and our calculations are done in that limit.

The stabilizing role of metabolism

Previous studies have emphasized a possible stabilizing role of allometric scaling [26]. Since predators are larger than their prey, with a median size ratio $M \approx 80$ [51], allometric scaling $m_i \sim W_i^{-\beta}$ suggests that they should have slower metabolism, $m \approx 0.3$ for $\beta = 1/4$. These studies have shown that this favors stability and coexistence in dynamical simulations of complex food webs.

Our food chain model reaches a similar conclusion, with a simple explanation. Consumer-driven consumption gives $\lambda \sim m$ (Box 1). Therefore, lowering m reduces the strength of top-down feedbacks, which leads to greater stability (Fig. 3 and 4). On the other hand, for resource-driven consumption, we obtain the opposite conclusion: $\lambda \sim 1/m$ and slower consumers *destabilize* the system.

Of these two scalings for consumption rates, each is supported by one of the empirical examples above (herbivory or cascade strength in tritrophic chains). Furthermore, despite predators being larger than their prey, there is no overall tendency for them to have a slower metabolism, as we show in data compiled from multiple studies (Fig. S3 to S5). Therefore, it may be that different ecological settings favor either slower or faster consumer metabolism.

DISCUSSION

Our understanding of many ecological phenomena relies on intuitions developed from simple food chains. Despite its fundamental role, this field has become increasingly fragmented. On the one hand, functioning and stability patterns, such as biomass pyramids and trophic cascades, have often been studied from different premises. In particular, various energetic and dynamical models have relied on conflicting assumptions, as we clarified by embedding them in the same formalism.

On the other hand, studies have tended to emphasize the role of one among a list of key ecological parameters: primary productivity g, predator-prey body metabolic ratio m, biomass conversion efficiency ε or interaction strength a. We have shown here that the action of these parameters can only be understood in conjunction, yet their main interplay is also simple: it can be summarized in a concise map with two main axes.

The first synthetic parameter, $\lambda = m\varepsilon a^2$, determines the presence of top-down control in the chain, via the strength of a trophic level's feedback on itself through its predators (Fig. 1c). The second synthetic parameter $\kappa = \varepsilon/m$ controls the overall top-heaviness of the biomass distribution, but has no effect on essential stability properties (Fig. 3 and 4). Counter-intuitively, top-heavy distributions do not imply strong top-down control: species with more efficient assimilation and slower turnover can acquire and store larger amounts of energy, without necessarily exerting stronger pressure on lower levels.

The bottom-up regime ($\lambda < 1$) is characterized by (regular or inverted) pyramidal patterns in various functioning and stability metrics, replaced by cascade patterns in the top-down regime ($\lambda > 1$).

A third parameter, $\rho = r/g$, modulates these patterns without creating qualitatively new regimes. It represents the energy lost to mortality and metabolic costs, and intervenes only as long as it is an important limiting factor. When $\rho \ll 1$ (low costs r or high primary productivity g), its precise value becomes irrelevant to any food chain dynamics. This may explain conflicting empirical findings on whether primary productivity is a predictor of effects such as trophic cascade strength [5, 6].

These results provide an intuitive basis for understanding relationships observed in data or complex simulations, and advancing our understanding of a number of standing paradoxes. We have shown that they could be used to test quantitative predictions on empirical relationships between consumption, metabolism and trophic cascade strength. They must yet be developped further and complemented with extensive data in order to provide a rigorous testing ground for food chain theory.

Self-regulation and functional response

We have shown that self-regulation is at the heart of the disagreement between the energetic and dynamical approaches (Box 1). By curtailing consumer growth before resource production is depleted, self-regulation stabilizes the dynamics, attenuates top-down cascades, and gives rise to bottom-up pyramidal patterns, where each level's biomass is fixed by its energy influx.

Many food web models, e.g. [26], do not admit explicit self-regulation in the form of density-dependent mortality D_i, except at the basal level. Nevertheless, they often contain predator interference [52] which is widely supported by empirical evidence [31, 33].

Interference plays a similar self-regulating role at equilibrium. For instance, this can be seen in the dynamics of a consumer with a Type II functional response and predator interference,

$$\frac{1}{B_i}\frac{dB_i}{dt} = -r + \varepsilon \frac{\alpha B_{i-1}}{1 + \underbrace{IB_i}_{\text{Interference}} + \underbrace{H\alpha B_{i-1}}_{\text{Handling}}} \tag{24}$$

where I is the interference strength and H is the handling time. Notice that, at equilibrium (setting both sides to zero), this is equivalent to

$$0 = -r - (rI)B_i + (\varepsilon - rH)\alpha B_{i-1} \tag{25}$$

the top predator equilibrium condition in a Lotka-Volterra model (3) with self-regulation $D = rI$ and a

reduced conversion efficiency $\varepsilon - rH$. Thus, whenever interference I can be measured, it is in principle possible to estimate self-regulation D.

This strict mathematical identity between different functional responses at equilibrium does not hold in all generality, as it requires neglecting predation mortality in (24). But more qualitatively, our results are expected to remain relevant as long as some form of density dependence stabilizes the dynamics [33, 53].

In more complex food web models, even the premise of a robust equilibrium description can become tied to self-regulation. Dynamics may otherwise become excitable and oscillatory or chaotic [22] unless species satisfy complex conditions [54–56]. In these unstable regimes, even qualitative conclusions can be sensitive to model details.

Pattern regularity and coherence

Coherent patterns, from pyramids to cascades, have been identified here under the assumption that the parameters λ and κ are constant throughout the chain, owing to equations (4) and (5).

Two factors weigh strongly against this simplfying assumption. First, instead of scaling with the same metabolic rate m_i, ecological processes may exhibit different scalings. Their relative importance would be increasing or decreasing through the chain, perhaps creating mixed patterns such as a biomass "barrel" [57].

Second, many chains involve organisms belonging to distinct taxonomic classes, with vastly different physiologies. Direct and model estimates of biomass conversion efficiency ε often put it around $10 - 20\%$ [25, 58–60] but it could vary over at least an order of magnitude, and is expected to be lower for herbivores than carnivores [26].

More strikingly, data compiled from multiple studies (Fig. S3 to S5) reveals that the metabolic ratio m varies over four order of magnitudes, $m \in [10^{-2}, 10^{2}]$, in thousands of predator-prey pairs. While the body size ratio M exhibits a clear skew toward larger predators, the metabolic ratio m has no such skew: faster and slower consumers are equally common in the dataset, with significant variation between and within taxonomic classes. There may be no "typical" cross-ecosystem value of m (and hence λ and κ) to use as a baseline in models.

Finally, the effective interaction strength $a = \alpha/D$ could also vary within a food chain, although we lack data to estimate its range of variation. Few studies reliably quantify the absolute interaction strength α [30], and fewer provide estimates of self-regulation D [31]

These heterogeneities between levels may not allow food chains to retain clear pyramidal or cascade structures, and even if we observe such structures, they may not be robust to changes such as losing or adding one trophic level [23, 35]. This blurring of trophic patterns could explain some of the lack of consensus surrounding their general validity.

Still, phenomena such as trophic cascades are well-attested in various ecosystems, see e.g. [5, 46, 61]. This suggests that the food chain approach may remain valid in some limits: either for particular sets of species, or for averages over large communities.

One last issue is the possibility that some patterns could have causes outside the studied community. External energy subsidies, e.g. influxes of organic matter, or a predation range coupling multiple local communities, may be responsible for stronger trophic cascades [62] and top-heavy distributions [14, 63].

We believe that the only robust way to test these hypotheses is to combine different lines of evidence. For instance, the steep size spectrum of the fish community in Fig. 2a is incompatible with an inverted pyramid, but may indicate a cascade structure. In that case, the smaller fish must undergo intense predation, while the larger ones are weakly depleted. Predator removal experiments can be used to test the impact of predation. If they contradict this picture, the observed size spectrum may have no consistent explanation involving only the local food chain. Thus, by juxtaposing different functioning and stability properties, one can see whether they display consistent patterns, or whether some may indeed be shaped by external influences.

Conclusions and prospects

We have synthesized the basic predictions of food chain theory on a simple two-dimensional map, whose axes combine physiological and ecological properties. This map is divided in two regions, characterized by pyramidal and cascade structures in a variety of functioning and stability patterns. Using these predictions has allowed us to shed light on multiple empirical observations such as size spectra and trophic cascade strength.

If the predictions developped here are to hold in large ecological communities, they must be robust to the addition of diversity and structure within trophic levels, and to the presence of omnivory. There are theoretical grounds to expect that the simplified structure described here will retain an important predictive role in diverse communities [64], as we hope to show in future work.

Finally, we emphasize the need for consistency between functioning and stability patterns that have been studied extensively but independently from each other. This synthesis has been called for in conceptual frameworks [24], but it must become quantitative if it is to solve long-standing empirical paradoxes. The relationships that we have summarized here can become the basis for a systematic toolbox to get better insight into the trophic structure of an ecosystem.

ACKNOWLEDGMENTS

We thank J.-F. Arnoldi, N. Galiana Ibáñez, A. Sentis and Y. Zelnik for discussions during the elaboration of the manuscript. Our gratitude goes to A. Makarieva, C. White, E. Sala and their respective coauthors and sources for the data they compiled or collected, as well as all scientists who generously shared their work on the open GloBI and FishBase databases. This work was supported by the TULIP Laboratory of Excellence (ANR-10-LABX-41) and by the BIOSTASES Advanced Grant, funded by the European Research Council under the European Union's Horizon 2020 research and innovation programme (666971).

[1] C. S. Elton, *Animal ecology* (University of Chicago Press, 1927).
[2] S. D. Fretwell, Oikos , 291 (1987).
[3] M. Loreau, *From populations to ecosystems: Theoretical foundations for a new ecological synthesis (MPB-46)* (Princeton University Press, 2010).
[4] N. G. Hairston, F. E. Smith, and L. B. Slobodkin, The american naturalist **94**, 421 (1960).
[5] M. L. Pace, J. J. Cole, S. R. Carpenter, and J. F. Kitchell, Trends in ecology & evolution **14**, 483 (1999).
[6] F. Micheli, Science **285**, 1396 (1999).
[7] J. M. Chase, Trends in ecology & Evolution **15**, 408 (2000).
[8] D. R. Strong, Ecology **73**, 747 (1992).
[9] J. B. Shurin and E. W. Seabloom, Journal of Animal Ecology **74**, 1029 (2005).
[10] E. Borer, E. Seabloom, J. Shurin, K. Anderson, C. Blanchette, B. Broitman, S. Cooper, and B. Halpern, Ecology **86**, 528 (2005).
[11] J. W. Fox, Oikos **116**, 189 (2007).
[12] J. B. Shurin, D. S. Gruner, and H. Hillebrand, Proceedings of the Royal Society of London B: Biological Sciences **273**, 1 (2006).
[13] B. D. Fath and M. C. Killian, Ecological Modelling **208**, 286 (2007).
[14] D. J. McCauley, G. Gellner, N. D. Martinez, R. J. Williams, S. A. Sandin, F. Micheli, P. J. Mumby, and K. S. McCann, Ecology letters (2018).
[15] C. B. Woodson, J. R. Schramski, and S. B. Joye, Nature communications **9**, 23 (2018).
[16] R. L. Lindeman, Ecology **23**, 399 (1942).
[17] A. M. Hemmingsen, Reports of the Steno Memorial Hospital (Copenhagen) **13**, 1 (1960).
[18] U. Borgmann, Canadian Journal of Fisheries and Aquatic Sciences **44**, s136 (1987).
[19] R. Trebilco, J. K. Baum, A. K. Salomon, and N. K. Dulvy, Trends in ecology & evolution **28**, 423 (2013).
[20] A. J. Lotka, *Elements of mathematical biology* (Dover Publications, 1956).
[21] V. Volterra, ICES Journal of Marine Science **3**, 3 (1928).
[22] K. S. McCann, *Food webs (MPB-50)* (Princeton University Press, 2011).
[23] T. Jonsson, Scientific Reports **7**, 10912 (2017).
[24] M. A. Leibold, J. M. Chase, J. B. Shurin, and A. L. Downing, Annual review of ecology and systematics **28**, 467 (1997).
[25] K. H. Andersen, J. Beyer, and P. Lundberg, Proceedings of the Royal Society of London B: Biological Sciences **276**, 109 (2009).
[26] U. Brose, R. J. Williams, and N. D. Martinez, Ecology letters **9**, 1228 (2006).
[27] M. L. Rosenzweig, Science **171**, 385 (1971).
[28] S. J. McNaughton, M. Oesterheld, D. A. Frank, and K. Williams, Nature **341**, 142 (1989).
[29] S. Jennings, J. d. Oliverai, and K. J. Warr, Journal of Animal Ecology **76**, 72 (2007).
[30] E. L. Berlow, A.-M. Neutel, J. E. Cohen, P. C. De Ruiter, B. Ebenman, M. Emmerson, J. W. Fox, V. A. Jansen, J. Iwan Jones, G. D. Kokkoris, *et al.*, Journal of animal ecology **73**, 585 (2004).
[31] G. T. Skalski and J. F. Gilliam, Ecology **82**, 3083 (2001).
[32] J. Cebrian and C. Duarte, Functional Ecology **8**, 518 (1994).
[33] I. A. Hatton, K. S. McCann, J. M. Fryxell, T. J. Davies, M. Smerlak, A. R. Sinclair, and M. Loreau, Science **349**, aac6284 (2015).
[34] M. E. Power, Ecology **73**, 733 (1992).
[35] E. Teramoto, Ecological modelling **69**, 135 (1993).
[36] T. Cheon, Physical review letters **90**, 258105 (2003).
[37] R. Trebilco, N. K. Dulvy, S. C. Anderson, and A. K. Salomon, Proceedings of the Royal Society of London B: Biological Sciences **283**, 20160816 (2016).
[38] H. Cyr and M. L. Pace, Nature **361**, 148 (1993).
[39] J. B. Shurin, E. T. Borer, E. W. Seabloom, K. Anderson, C. A. Blanchette, B. Broitman, S. D. Cooper, and B. S. Halpern, Ecology letters **5**, 785 (2002).
[40] A. M. Makarieva, V. G. Gorshkov, B.-L. Li, S. L. Chown, P. B. Reich, and V. M. Gavrilov, Proceedings of the National Academy of Sciences **105**, 16994 (2008).
[41] C. R. White and R. S. Seymour, Proceedings of the National Academy of Sciences **100**, 4046 (2003).
[42] D. S. Glazier, Functional Ecology **23**, 963 (2009).
[43] J.-F. Arnoldi, M. Loreau, and B. Haegeman, Journal of Theoretical Biology **389**, 47 (2016).
[44] J.-F. Arnoldi and B. Haegeman, in *Proc. R. Soc. A*, Vol. 472 (The Royal Society, 2016) p. 20150874.
[45] J.-F. Arnoldi, A. Bideault, M. Loreau, and B. Haegeman, Journal of theoretical biology **436**, 79 (2018).
[46] D. A. Jessup, M. Miller, J. Ames, M. Harris, C. Kreuder, P. A. Conrad, and J. A. Mazet, EcoHealth **1**, 239 (2004).
[47] D. Shanafelt and M. Loreau, Unpublished.
[48] D. L. DeAngelis, R. Goldstein, and R. O'Neill, Ecology **56**, 881 (1975).
[49] K. McCann and P. Yodzis, Ecology **75**, 561 (1994).
[50] O. J. Schmitz, P. A. Hambäck, and A. P. Beckerman, The American Naturalist **155**, 141 (2000).
[51] U. Brose, T. Jonsson, E. Berlow, P. Warren, C. Banasek-Richter, L. Bersier, J. Blanchard, T. Brey, S. Carpenter, M. Blandenier, *et al.*, Ecology **87**, 2411 (2006).
[52] J. R. Beddington, The Journal of Animal Ecology , 331 (1975).
[53] K. Kawatsu and M. Kondoh, Proc. R. Soc. B **285**, 20180698 (2018).
[54] H. Freedman and J.-H. So, Mathematical biosciences **76**, 69 (1985).
[55] R. Redheffer and Z. Zhiming, Nonlinear Analysis: Theory, Methods & Applications **5**, 1309 (1981).

[56] R. Redheffer and W. Walter, Journal of differential equations **52**, 245 (1984).
[57] T. Jonsson, J. E. Cohen, and S. R. Carpenter, Advances in ecological research **36**, 1 (2005).
[58] D. Pauly and V. Christensen, Nature **374**, 255 (1995).
[59] H. E. Welch, Ecology **49**, 755 (1968).
[60] C. P. Madenjian, R. J. Hesselberg, T. J. DeSorcie, L. J. Schmidt, R. M. Stedman, R. T. Quintal, L. J. Begnoche, and D. R. Passino-Reader, Environmental science & technology **32**, 886 (1998).
[61] B. Worm and R. A. Myers, Ecology **84**, 162 (2003).
[62] S. J. Leroux and M. Loreau, Ecology letters **11**, 1147 (2008).
[63] P. A. Del Giorgio, J. J. Cole, N. F. Caraco, and R. H. Peters, Ecology **80**, 1422 (1999).
[64] M. Barbier, J.-F. Arnoldi, G. Bunin, and M. Loreau, Proceedings of the National Academy of Sciences **115**, 2156 (2018).